Binding of the Fluorescent Substrate Analogue 2′,3′-*O*-(2,4,6-Trinitrophenylcyclohexadienylidene)adenosine 5′-Triphosphate to the Gastric H^+,K^+-ATPase: Evidence for Cofactor-Induced Conformational Changes in the Enzyme†

Larry D. Faller

The Center for Ulcer Research and Education, Department of Medicine, University of California at Los Angeles School of Medicine and Veterans Administration Hospital Center, Los Angeles, California 90073

Received October 3, 1989; Revised Manuscript Received November 27, 1989

ABSTRACT: TNP-ATP binds to the gastric H,K-ATPase with a 4.6-fold increase in fluorescence intensity and 10-nm blue shift that indicate a relatively hydrophobic protein environment. The fluorescence enhancement saturates and is compatible with binding to a single class of specific nucleotide sites with K_d < 25 nM and $N = 3.4 \pm 0.9$ nmol mg^{-1}. Cofactors of the H,K-ATPase affect the fluorescence enhancement. K^+ causes a rapid fluorescence quench by binding to a single class of sites with K_d = 3 mM. Mg^{2+} rapidly and completely reverses the K^+ quench and then causes a slow fluorescence quench. The maximum enhancement is approximately halved by either Mg^{2+} or K^+ in titrations with both protein and fluorophore. Therefore, TNP-ATP reports changes in protein environment compatible with cofactor-induced changes in the conformation of the enzyme.

The magnesium-dependent, hydrogen ion transporting, and potassium-stimulated adenosinetriphosphatase (EC 3.6.1.3) (H,K-ATPase)[1] responsible for acid secretion across the gastric epithelium is mechanistically and structurally related to the enzymes that actively transport sodium and calcium ions across other membranes in mammalian tissues. All three of these enzymes catalyze ATP hydrolysis by forming a phosphoenzyme intermediate. The reactive amino acid in each case is aspartic acid, and the covalently modified polypeptides each contain about 1000 amino acids. Their primary structures were solved recently (Shull et al., 1985; MacLennan et al., 1985; Shull & Lingrel, 1986). Many of the amino acids are conserved, including those surrounding the aspartate directly involved in catalysis (Walderhaug et al., 1985) and residues in sequences that are believed to form the three-dimensional site on the native, folded protein that recognizes substrate (Farley & Faller, 1985).

How these enzymes carry out transport, as well as catalysis, is unknown. The two most fundamental and important unsolved problems are, first, how the energy released from ATP by hydrolysis is coupled to transport and, second, how ions are physically translocated. The solution to both problems is thought to depend on the existence of two enzyme conformations (Tanford, 1983), and the conformational model is so widely accepted that the sodium, potassium, and proton pumps are referred to as E_1E_2-type ATPases. An ion pump can be devised from two enzyme conformations, if the ion binding sites are on different sides of the membrane and have different affinities for the transported ions in the two conformers. The pump will be ATP-driven if one conformer (E_1) can react only with ATP and the other conformer (E_2) only with P_i (Jencks, 1980). Therefore, it is important to demonstrate the existence of different enzyme conformations and test predictions of the model. For example, the conformational equilibrium should be shifted by transported ions binding to the different conformers with unequal affinity.

One experimental approach to the study of enzyme conformational equilibria has been the use of fluorescent substrate analogues to report ion-induced changes in the protein environment of the bound probe. 2′,3′-*O*-(2,4,6-Trinitrophenylcyclohexadienylidene)adenosine 5′-triphosphate (TNP-ATP) is a fluorescent analogue of ATP (Hiratsuka & Uchida, 1973) that has been used extensively to investigate both the sodium (Moczydlowski & Fortes, 1981) and calcium (Dupont et al., 1982; Wanatabe & Inesi, 1982) pumps. Sartor has shown the feasibility of using TNP-ATP to probe nucleotide sites on the gastric H,K-ATPase as well (Sartor et al., 1982). Preliminary evidence for weaker binding of the fluorophore in the presence of K^+ and an additional class of TNP-ATP sites in the presence of Mg^{2+} was reported. These observations could result from conformational changes and have important implications not only for the mechanism of the H,K-ATPase but, by extension, for theoretical models of transport by the E_1E_2 class of ATPase. Therefore, a systematic reinvestigation of TNP-AXP binding to the gastric enzyme was undertaken. Some results of this study have been communicated in preliminary form (Faller, 1986) and in a recent paper (Faller, 1989a).

Experimental Procedures

Materials

H,K-ATPase. The enzyme is found in vesicles isolated from the gastric mucosae of a variety of mammals (Ganser & Forte, 1973). H,K-ATPase prepared by a step-gradient method (Chang et al., 1977) was used in this study. The fundic region of hog stomachs was scraped, and the cell contents were re-

†This work was supported by National Science Foundation Grant DMB 83-09756 and by U.S. Public Health Service Grants DK 36873 and section C2 of Program Project AM 17328 (George Sachs, overall principal investigator).

[1] Abbreviations: H,K-ATPase, Mg^{2+}-dependent, H^+-transporting, and K^+-stimulated ATPase (EC 3.6.1.3); Na,K-ATPase, Mg^{2+}-dependent and Na^+- and K^+-stimulated ATPase; Ca-ATPase, Ca^{2+}- and Mg^{2+}-dependent ATPase; SR, sarcoplasmic reticulum; TNP-AXP, 2′,3′-*O*-(2,4,6-trinitrophenylcyclohexadienylidene)ATP or -ADP; FITC, fluorescein 5′-isothiocyanate; eosin Y, 2′,4′,5′,7′-tetrabromofluorescein.

0006-2960/90/0429-3179$02.50/0

leased by homogenization. The microsomal fraction was separated by differential centrifugation and fractionated further by sedimenting for 2 h at 59 000 rpm on a discontinuous density gradient in a Beckman Z60 zonal rotor. The vesicles recovered from the 0.25 M sucrose (60–80 mL)–7% (w/w) Ficoll interface (lighter fraction) are activated by K^+ and catalyze ATP hydrolysis with coupled proton transport. To assure free access of ions to both sides of the membrane for the experiments described, the vesicles were ruptured by suspending in water, freezing, lyophilizing, and storing at −80 °C. The specific activity of the five enzyme preparations used in this study was 176 ± 47 μmol of ATP hydrolyzed/(h·mg of protein), when protein content was determined by the Lowry method using bovine serum albumin standards (Lowry et al., 1951). The phosphorylation capacity of the enzyme preparation is 1.5 ± 0.3 nmol mg^{-1} (Faller et al., 1983).

A variety of criteria have been used to ascertain the purity of the enzyme. More than 75% of the protein in vesicles prepared by the described method forms a single band on sodium dodecyl sulfate–polyacrylamide gels, corresponding to a molecular weight of about 100 000 (Chang et al., 1977). Solubilization might be expected to remove smaller peptides and increase the specific activity. The specific activity of enzyme from the 7% Ficoll–34% sucrose (heavier) fraction did approximately double when solubilized with *n*-octyl glucoside and reconstituted into liposomes (Rabon et al., 1985). However, the heavier fraction is only about half as active as the lighter fraction to begin with, so the final specific activity of the reconstituted enzyme fell within the range cited for the five enzyme preparations used in this study. Therefore, there is no evidence that solubilization produces purer H,K-ATPase.

Homogeneity of the enzyme's nucleotide binding and catalytic properties is of particular concern in interpreting the experiments that will be reported. ATP-protectable labeling of the preparation by FITC occured on a single peptide (Farley & Faller, 1985). At each pH in the range 5.5–8.0 a single partition coefficient describes catalysis of ^{18}O exchange between inorganic phosphate and water by the terminal steps in the reaction pathway (Faller, 1989b). Moreover, there is direct proportionality between the specific ATPase activity of the preparation and the rate of isotope exchange (Faller & Elgavish, 1984). Therefore, any low molecular weight impurities in the preparation, or unreactive 100K polypeptides, do not affect substrate binding, or turnover, by the functional enzyme molecules.

Reagents. TNP-ATP and TNP-ADP were purchased from Molecular Probes. Their concentrations were determined spectrophotometrically at 408 nm by using an extinction coefficient of 2.64×10^4 M^{-1} cm^{-1}. All other reagents were the highest grade available.

Methods

Fluorescence Measurements. Fluorescence measurements were made in a Perkin-Elmer MPF 44 spectrofluorimeter with the entrance and exit slit widths set at 10 nm. TNP-AXP was excited at 405 nm. The amount of scattered light reaching the detector was reduced by placing a yellow Corning CS 3-70 cutoff filter after the sample. A high-intensity cell holder was also required for detection of the emitted light at 546 nm. The design of the high-intensity cell holder makes it difficult to thermostat, or use with a magnetic stirrer. Therefore, the measurements were made at ambient temperature, and the homogeneity of vesicle suspensions was maintained with a Spectrocell paddle-type stirrer fitted into the top of a 1-cm^2 cuvette. Experimentally, emission from the fluorophore was stable and was unaffected by briefly opening and closing the cell compartment, alternately closing and opening the shutter, or turning the stirrer off and on. Any effect on measured parameters of different ambient temperatures on different days is reflected in the quoted standard deviations.

Fluorescence titrations were carried out by successively adding small aliquots of titrant and scanning through the emission maximum. After correction for dilution by titrant, the observed fluorescence (F_{obs}) is

$$F_{obs} = (Q[L]_0 + RP_0) + (Q/2)(\gamma - 1)\{([L]_0 + NP_0 + K_d) - [([L]_0 + NP_0 + K_d)^2 - 4NP_0[L]_0]^{1/2}\} \quad (1)$$

when a fluorescent ligand (L) binds to a single class of protein (P) sites (Appendix). The subscript zero denotes the total, measured concentrations of the independent variables L and P, the latter expressed in μg mL^{-1}.

The first term in parentheses on the right-hand side of eq 1 is the fluorescence that would be observed if fluorophore and protein were added to separate cuvettes and the measured intensities were summed. To reduce the number of estimated parameters, the fluorescence increment (Q) and the scattering coefficient (R) were evaluated from control experiments in which titrant was added to buffer. Actually, the fluorecence intensity does not remain proportional to fluorophore concentration as the fluorophore concentration is raised, because an increasing amount of the exciting light is absorbed before it reaches the volume element from which emission is observed. The polynominal expression

$$F_{free} = Q[L]_0 - Q'[L]_0^2 \quad (2)$$

was used to correct for this inner-filter effect. The base line is also curved when protein is the titrant, presumably because the intensity of light incident on the observed volume element is reduced by increased light scattering at higher vesicle concentrations. The curvature in the base line of titrations with protein was handled empirically by expressing $F_{scatter}$ as a polynominal:

$$F_{scatter} = RP_0 - R'P_0^2 \quad (3)$$

Increased scattering did not introduce an artifact by reducing the measured emission, because the difference between the fluorescence intensity from a cuvette containing TNP-ATP, enzyme, and enough $H_2VO_4^-$ to prevent TNP-ATP binding (Faller, 1989a) and the signal from a cuvette containing TNP-ATP and enzyme alone was constant within 10% and equal to the emission of the free fluorophore over the entire range of protein concentrations.

The second term on the right in eq 1 is the enhancement (E) that results from fluorophore binding to the protein. The parameters that characterize the binding are the enhancement factor (γ), the site stoichiometry (N), and the fluorophore dissociation constant (K_d). They were estimated by a derivative-free, nonlinear least-squares fit of eq 1 to the experimental data (T. J. Reedy and L. D. Faller, unpublished results).

Results

TNP-ATP Binding to Apoenzyme. When TNP-ATP is added to vesicular H,K-ATPase with 0.8 mM EDTA present (apoenzyme), the resulting fluorescence is greater than the summed contributions of fluorophore and enzyme (Figure 1). Millimolar EDTA chelates Mg^{2+} and prevents phosphorylation of H,K-ATPase by either ATP (Wallmark & Mardh, 1979) or P_i (Faller & Elgavish, 1984). Therefore, neither divalent cation nor phosphorylation is required for TNP-ATP binding. One indication TNP-ATP binding is specific is that ATP

Table I: Summary of Parameters for TNP-ATP Binding to a Single Class of Sites[a]

cofactor	time	titrant	n	K_d (nM)	γ	N (nmol mg^{-1})	RRMSE[b] (%)
		L[c]	11	<25	5.0 ± 0.8	3.2 ± 0.6	5.0
		P[d]	10	<25	4.2 ± 1.3	3.6 ± 1.2	3.6
		L + P	21	<25	4.6 ± 1.0	3.4 ± 0.9	4.3
7 mM K^+		L + P	3	<25	2.7 ± 0.3	4.3 ± 1.0	4.3
2.8 mM Mg^{2+}	initial	L + P	2	<25	4.4 ± 1.7	2.7 ● 0.8	6.2
	final	L + P	2	<25	2.5 ± 0.9	3.2 ± 0.2	14.8

[a] Mean value ± standard deviation estimated by eq 1. Experimental conditions: 0.8 mM EDTA and 40 mM Tris-HCl at pH 7.4 and ambient temperature. [b] Root mean square error expressed relative to the maximum enhancement. [c] Q = 37.2 ± 6.4 μM^{-1} and Q' = 5.6 ± 3.7 μM^{-2} (n = 7). P_0 = 60, 120, or 180 μg^{-1} mL. [d] R = 0.341 ± 0.075 μg^{-1} mL and R' = (1.68 ± 0.60) × 10^{-4} μg^{-2} mL^2 (n = 6). $[L]_0$ = 0.33, 0.66, or 1.31 μM.

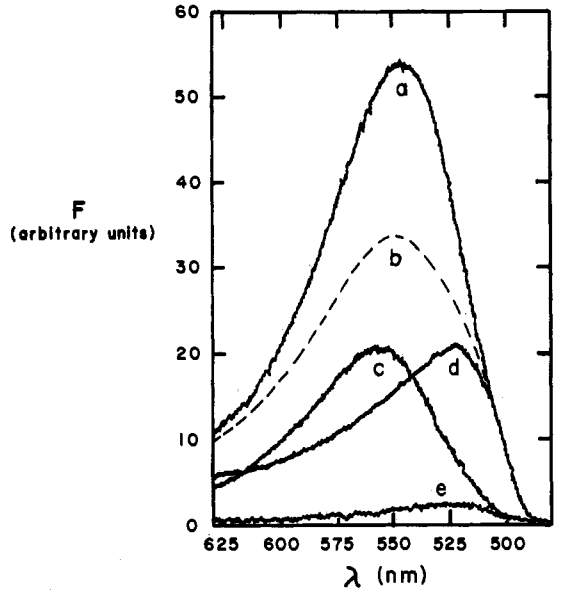

FIGURE 1: Binding to the H,K-ATPase enhances TNP-ATP fluorescence. The fluorescence intensity of bound TNP-ATP (a, emission maximum 546 nm) is greater than the calculated sum (b, dashed line) of the fluroescence of free fluorophore (c, emission maximum 556 nm) and the contribution of light scattering from gastric microsomal vesicles to the signal (d, peak at 522 nm). Curve e is the base line. Light of 405-nm wavelength was used to excite TNP-ATP. Other conditions: 2 μM TNP-ATP, 120 μg mL^{-1} protein, 0.8 mM EDTA, and 40 mM Tris-HCl buffer at pH 7.4 and ambient temperature.

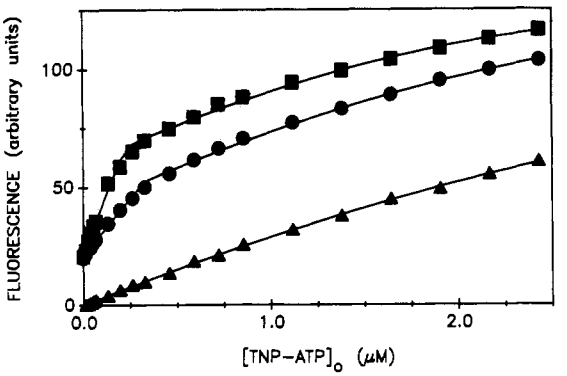

FIGURE 2: Titration of protein with fluorophore. The uppermost points (squares) are the observed fluorescence intensities when 60 μg mL^{-1} protein was titrated with TNP-ATP in 0.8 mM EDTA and 40 mM Tris-HCl at pH 7.4 and ambient temperature. KCl (7 mM) was also present in the middle curve (circles). The theoretical lines were calculated to test the hypothesis that TNP-ATP binds to a single class of protein sites. The values of the parameters in eq 1 that give the illustrated fits are reported in Table I. The lowest curve (triangles) is a separate, control experiment in which TNP-ATP was added to buffer. The fluorescence of free fluorophore was estimated by eq 2. The fluorescence increments describing the base line are given in footnote c of Table I.

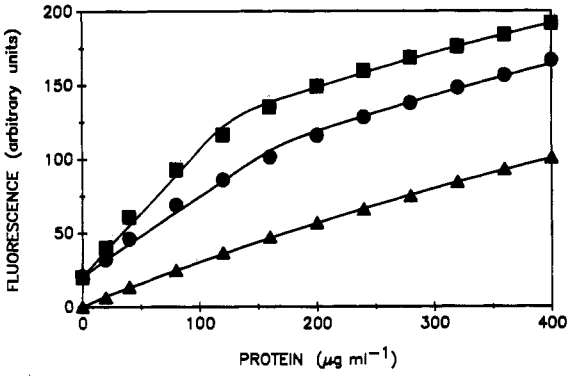

FIGURE 3: Titration of fluorophore with protein. In the uppermost curve (squares) 0.8 μM TNP-ATP was titrated with H,K-ATPase. The middle curve (circles) was measured in 7 mM KCl. The theoretical lines are the fits given by the parameters recorded in Table I to eq 1. The lowest curve (triangles) shows the contribution of scattering to the observed signal. The scattering coefficients defined in eq 3 are given in footnote d of Table I. Other experimental conditions are given in the legend to Figure 2.

reverses the fluorescence enhancement (Faller, 1989a). Another is that the fluorescence enhancement saturates at low concentrations of TNP-ATP.

(*A*) *Saturation.* The upper curve in Figure 2 is a representative titration of apoenzyme with TNP-ATP. The lower curve is a typical control experiment in which TNP-ATP was added to buffer. The best estimates of Q and Q', inferred from seven control titrations are given in footnote c of Table I. They were fixed when fitting eq 1, modified to include the ligand-squared term (eq 2), to data from titrations of H,K-ATPase with TNP-ATP. The mean values of the remaining parameters, deduced from 11 titrations of gastric vesicles with TNP-ATP, are summarized on row 1 of Table I.

Binding is immeasurably tight. That is, the estimated dissociation constants (K_d) were all within 1 standard deviation of zero. The largest value estimated for any of the titration curves is cited in the table as a reasonable estimate for the maximum value of K_d. Three different fixed amounts of protein were titrated with TNP-ATP (footnote c, Table I). The maximum fluorescence change was approximately proportional to the protein concentration, which is evidence that all the binding sites were filled. The ligand concentrations required to saturate the enzyme were roughly equivalent to the enzyme concentrations calculated by using the molecular weight deduced from the primary structure of the enzyme (Shull & Lingrel, 1986). Therefore, at most one TNP-ATP molecule binds per 114K polypeptide. Immeasurably tight and stoichiometric binding is strong evidence for specific binding.

(*B*) *Enhancement Factor.* It is reasonable to assume that all the ligand is eventually bound when protein is the titrant. Therefore, the ratio of the emitted light intensity at the end of the titration, corrected for scattered light, to the initial intensity equals the enhancement factor (γ). In practice, the end point of the titration may not be reached. Nevertheless,

a lower estimate of γ that is independent of binding model can be made from initial and final fluorescence levels. The value estimated for TNP-ATP binding to apo-H,K-ATPase was 4.8 ± 0.8 (n = 10).

The upper curve in Figure 3 shows a typical titration of TNP-ATP with apoenzyme. The lower curve is the control titration in which gastric microsomal vesicle fragments were added to buffer. Six control titrations gave the estimates of R and R' recorded in footnote d of Table I. The contribution of light scattering to F_{obs} was treated as known in fitting titrations of fluorophore with gastric vesicles to eq 1, modified to include a protein-squared term. The estimated parameters for TNP-ATP binding to a single class of apoprotein sites are summarized on row 2 of Table I. The estimated value of γ is in satisfactory agreement with the model-independent estimate from the observed initial and final fluorescence levels (4.8). The observed maximum enhancement was always within 15% of the estimated value. The value of γ estimated from titrations of protein with ligand (row 1) is the same, within the errors of their estimation, as the value of γ estimated from titrations of ligand with protein (row 2).

(*C*) *Stoichiometry.* The enhancement initially increases linearly with ligand concentration when gastric vesicles are titrated with TNP-ATP (Figure 2). This means essentially all of the fluorophore is bound and makes possible rough estimates of the stoichiometry from the total ligand concentration at which asymptotes to the initial and final experimental points intersect. The estimated value of N is 2.6 ± 0.7 nmol mg^{-1} (n = 11), in satisfactory agreement with the stoichiometry estimated by fitting eq 1 to titrations of enzyme with fluorophore (Table I, row 1, column 7). The same stoichiometry is estimated when protein is the titrant (Table I, row 2, column 7).

Additional evaluations of N can be made by combining data from the two types of titration (Reedy and Faller, unpublished results). Since all the sites are filled at the end point when ligand is titrant and all the ligand is bound at the end point when protein is titrant, the ratio of the maximum enhancements is related to N by the total concentrations of ligand and protein. Therefore, this ratio gives the stoichiometry directly when there is only one class of sites. N can also be obtained by combining the titrant concentrations that cause half the maximum enhancements ($[T]_{0,1/2}$). The value of N calculated from the ratio of maximum enhancements is 3.8 ± 1.1 nmol mg^{-1}, and the value derived from the half-maxima is 3.6 ± 0.7 nmol mg^{-1} (n = 5).

All the methods of estimating N give values within 1 standard deviation of each other. More complicated schemes than fluorophore binding to a single class of protein sites cannot be excluded, especially since binding is immeasureably tight. However, eq 1 satisfactorily describes the data. The predictions of the two types of titration are combined on row 3 of Table I to give best estimates of the parameters in eq 1. The best estimate of the stoichiometry for TNP-ATP binding to apo-H,K-ATPase is 3.4 ± 0.9 nmol mg^{-1}.

Cofactor-Induced Changes in the Fluorescence Enhancement. Mg^{2+}, which is required for catalysis and transport, and K^+, which accelerates ATP hydrolysis and is cotransported with H^+, cause changes in the fluoresence enhancement as shown in Figure 4. K^+ causes a rapid quench. Mg^{2+} completely and rapidly reverses the K^+ quench (Mg^{2+} enhancement), and then there is a slow Mg^{2+} quench which is not reversed by 8 mM EDTA. The Mg^{2+} quench also occurs in the absence of K^+. The fluorescence levels in the absence of metal ions (+EDTA), in the presence of K^+, and in the presence of Mg^{2+} alone, or of both Mg^{2+} and K^+, are all stable for a least 4 h. These different fluorescence intensities could be caused by changes in the fraction of sites filled with TNP-ATP, by changes in the number of sites, or by different protein environments of the noncovalently bound fluorophore.

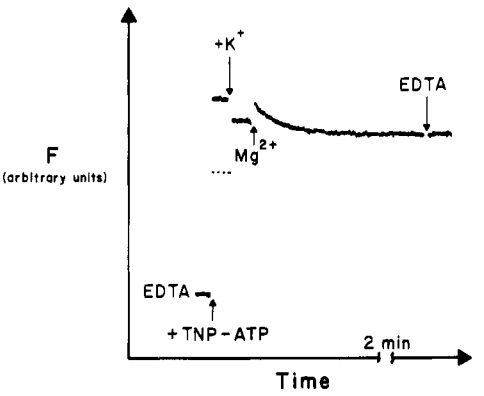

FIGURE 4: Metal cofactors of the H,K-ATPase change the protein environment of bound TNP-ATP. At the first arrow on the left, 0.8 μM TNP-ATP was added to 320 μg mL^{-1} protein in 0.8 mM EDTA. The dashed line is the contribution emission and light scattering from these concentrations of free fluorophore and microsomal vesicles make to the signal at 546 nm. At the second arrow the solution was made 7 mM in KCl and at the third arrow 2.8 mM in $MgCl_2$. Finally, the EDTA concentration was increased to 3.6 mM. The reasons for attributing most of the rapid K^+ quench, rapid Mg^{2+} enhancement, and slow Mg^{2+} quench to changes in enzyme conformation are explained in the text. Other conditions: 40 mM Tris-HCl at pH 7.4 and ambient temperature.

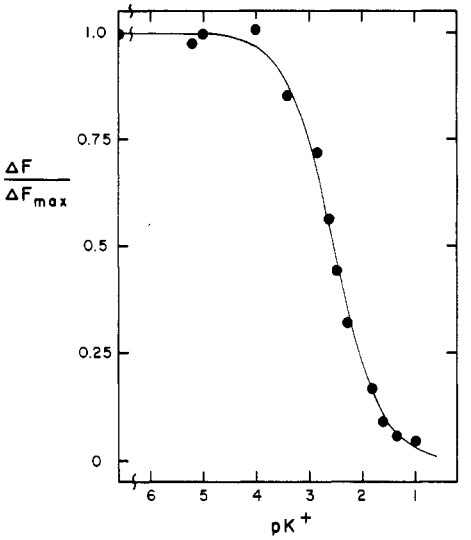

FIGURE 5: Titration of K^+ quench. Bound fluorophore was titrated with KCl. $pK^+ = -\log [K^+]$. The maximum quench was 55% of the enhancement. Fractional quench is plotted along the ordinate. The theoretical curve was calculated for K^+ binding to a single class of sites with dissociation constant 2.9 mM. Experimental conditions: 0.8 μM TNP-ATP, 320 μg mL^{-1} protein, 0.8 mM EDTA, and 40 mM Tris-HCl at pH 7.4 and ambient temperature.

(*A*) *K^+ Quench.* The half-time for the K^+ quench was shown to be less than 1.5 s by introducing a capillary into the fluorimeter, so that KCl could be added without removing the cuvette. The rapid K^+ quench can be titrated. The curve in Figure 5 was calculated for K^+ binding to a single class of sites with K_d = 2.9 mM. The maximum quench was 55% of the enhancement. NaCl had no effect on the fluorescence level. Therefore, the quench is caused by K^+ binding to a site, or class of sites, that is specific for the transported ion.

The middle curve in Figure 3 is a titration of TNP-ATP with gastric vesicles in the presence of 7 mM K^+. The same

TNP-ATP concentration was used to obtain the data in Figures 3 and 5. At the concentration of protein (320 μg mL^{-1}) titrated with K^+ (Figure 5), the titrations of TNP-ATP with apoprotein (squares) and K^+–protein complex (circles) are both complete (Figure 3). Therefore, essentially all of the fluorophore remains bound under conditions that cause about 70% of the quench. This is evidence that the lower fluorescence intensity measured in the presence of K^+ results from a different protein environment of bound fluorophore, rather than depopulation of sites. The decrease in enhancement factor was 30–40%, when estimated from the starting points and end points of titrations with protein in the absence and presence of K^+.

The middle curve in Figure 2 is a titration of gastric vesicles with TNP-ATP in the presence of 7 mM K^+. The maximum enhancement is about 40% less than the change observed with apoenzyme (upper curve). K^+ reduces the maximum enhancement by about the same percentage, regardless of whether ligand or protein is titrant. Therefore, K^+ does not significantly change the stoichiometry of TNP-ATP binding, because the ratio of the maximum enhancements in the two types of titrations, which is directly related to the stoichiometry, does not change. This evidence that the stoichiometry does not change strengthens the conclusion that the K^+ quench results principally from a lower enhancement factor.

The parameters estimated by fitting titrations in K^+ to eq 1 for binding to a single class of sites are reported on row 4 of Table I. The enhancement factor is approximately halved, but the stoichiometry of TNP-ATP binding is not significantly different. The dissociation constant in 7 mM K^+ could not be measured. However, a titration of gastric vesicles with TNP-ATP in 100 mM K^+ gave a K_d (86 ± 38 μM) statistically different from zero. By use of this value for K_d and assuming N = 3.4 nmol mg^{-1}, more than 85% of the fluorophore would still be bound at the end of the titration with K^+ shown in Figure 5. Although some dissociation cannot be excluded, the predominant effect of K^+ is to lower the yield of fluorescence from bound TNP-ATP.

(*B*) *Mg^{2+} Enhancement.* Mg^{2+} reverses the K^+ quench within the time required for manual addition of reagent into the stirred sample solution via a capillary (1.5 s). The fluorescence extrapolates back to the intensity observed with apoenzyme (Figure 4). Therefore, Mg^{2+} rapidly and completely reverses the K^+ quench.

(*C*) *Mg^{2+} Quench.* The rapid Mg^{2+} enhancement is followed by a slow Mg^{2+} quench (±K^+) with a half-time of 5–10 min. Neither effect is specific for Mg^{2+}. Ca^{2+}, which can also activate the enzyme (Faller & Elgavish, 1984), both rapidly reverses the K^+ quench and causes a slow quench. The slow quench could not be titrated with Mg^{2+} to learn about the metal binding site, because the enzyme preparation contains divalent cations and the same fluorescence decrease was observed when TNP-ATP was added to enzyme minus EDTA. Both divalent cation and substrate analogue are required for the slow quench, because it is not prevented by preincubation with either TNP-ATP or Mg^{2+}.

A logical explanation of this requirement for both Mg^{2+} and TNP-ATP would be that the Mg^{2+}-induced changes are caused by phosphorylation of the enzyme. However, phosphorylation cannot be the correct explanation for two reasons. First, the H,K-ATPase does not catalyze TNP-ATP hydrolysis (Faller, 1989a). Second, both the rapid Mg^{2+} enhancement and the slow Mg^{2+} quench are also observed with TNP-ADP.

Figures 6 and 7 show titrations in which Mg^{2+} was present. Titrant was not added serially in these experiments. Instead,

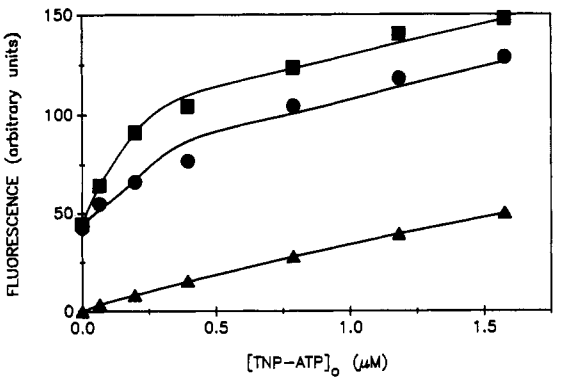

FIGURE 6: Titration of Mg^{2+}–enzyme with TNP-ATP. In this figure each titrant concentration is a separate experiment. The fluorescence change was initiated by adding different concentrations of TNP-ATP to a fixed amount of protein preincubated with Mg^{2+}. The squares in the uppermost curve are the initial fluorescence intensities found by extrapolating the observed emission back to time zero. The circles in the middle curve are the final intensities to which the fluorescence decayed after 5–10 min. The lowest curve (triangles) is the control experiment in which fluorophore was added to buffer. The lines through the experimental points were calculated with the parameters estimated by fitting eq 1 to the data. Other conditions: 120 μg mL^{-1} protein, 2.8 mM $MgCl_2$, 0.8 mM EDTA, and 40 mM Tris-HCl at pH 7.4 and ambient temperature.

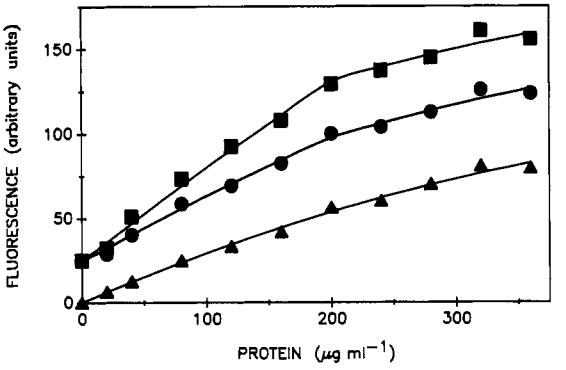

FIGURE 7: Titration of TNP-ATP with Mg^{2+}–enzyme. This titration was identical with the experiment explained in the legend to Figure 6, except that varying amounts of protein were incubated with Mg^{2+}, and the fluorescence change was initiated by adding the same aliquot of fluorophore each time to give a final TNP-ATP concentration of 0.66 μM. The bottom curve is the apparent emission at 546 nm before the fluorophore was added. The parameters estimated by fitting eq 1 to the data are reported in Table I.

each concentration point was obtained from a separate measurement. The fluorescence changes were initiated by adding TNP-ATP to different cuvettes, and the initial (squares) and final (circles) fluorescence intensities were recorded. The maximum enhancement decayed to about the same percentage of the initial level regardless whether fluorophore (Figure 6) or protein (Figure 7) was titrant. Therefore, the stoichiometry of TNP-ATP binding is not significantly affected by Mg^{2+}. The parameters estimated by fitting the data to eq 1 for binding to a single class of sites are reported on rows 5 and 6 of Table I. The enhancement factor is approximately halved by Mg^{2+} in the quenched state, but the stoichiometry of TNP-ATP binding is unaffected. Fluorophore binding is too tight for evaluation of the dissociation constant either before or after the slow quench.

Discussion

TNP-ATP binding to H,K-ATPase is characterized in this paper. The fluorescent substrate analogue has been used to count the number of nucleotide sites and report cofactor-mediated changes in the environment of bound fluorophore.

Characteristics of TNP-ATP Binding. TNP-ATP binding to apoenzyme enhances the fluorescence 4.6-fold (Table I) and shifts the emission maximum 10 nm to a shorter wavelength (Figure 1). This suggests that TNP-ATP binds to a hydrophobic region of the protein, since decreasing solvent polarity has been shown to increase the quantum yield and decrease the emission maximum of TNP-nucleotides (Hiratsuka, 1982). The enhancement fator for TNP-ATP binding to gastric vesicles (4.6) is only about half as large as the value reported for binding to Na,K-ATPase (Moczydlowski & Fortes, 1981), but it is not much different from values cited for TNP-ATP binding to Ca-ATPase which fall in the range 6–7 (Dupont & Pourgeois, 1983).

Binding is specific, because stoichiometric amounts of TNP-ATP saturate the enzyme (Figure 2). This conclusion is strenghtened by data showing, first, that ATP displaces TNP-ATP and, second, that TNP-ATP competitively inhibits the enzyme (Faller, 1989a). The last two observations also demonstrate that TNP-ATP binding is reversible. The simplest interpreation of all the data is that ATP and TNP-ATP compete for the same sites on the H,K-ATPase, although the alternative possibility of mutually exclusive binding to different sites cannot be excluded.

Equation 1 for binding to a single class of sites satisfactorily describes the titration data (Table I). More complicated schemes cannot be categorically ruled out, because TNP-ATP binds too tightly for numerical evaluation of the dissociation constant(s). However, there is indirect evidence from competition experiments for a single class of TNP-ATP sites (Faller, 1989a). First, TNP-ATP inhibits ATP hydrolysis with a single K_i, and second, ATP binds to apoenzyme and displaces TNP-ATP with a single apparent substrate constant. Two TNP-ATP affinities are not required to understand any of the experiments reported.

The best estimate of the TNP-ATP binding stoichiometry is 3.4 ± 0.9 nmol mg^{-1} (Table I), which is in good agreement with other tabulated estimates of the number of nucleotide sites on the H,K-ATPase (Faller, 1989a). The value found for N could mean there are two classes of substrate sites because only 1.5 ± 0.3 nmol mg^{-1} phosphoenzyme forms (Faller et al., 1983) under conditions where dephosphorylation is rate-limiting (Wallmark & Mardh, 1979).

Evidence for Cofactor-Induced Conformational Changes. The mechanism by which a cofactor affects the fluorescence of a reporter group reversibly bound to a single class of sites can be diagnosed by titrating with both ligand and protein, plus and minus the cofactor (Reedy and Faller, unpublished results). In the present instance the analysis is restricted to effects of Mg^{2+} and K^+ on the observed maximum enhancements, because TNP-ATP binding to the H,K-ATPase is too tight to resolve any change in the titrant concentration that causes half-maximum response. Nevertheless, a unique interpretation is possible. Both K^+ (Figures 2 and 3) and Mg^{2+} (Figures 6 and 7) reduce the maximum enhancement observed when either TNP-ATP or H,K-ATPase is titrant. A change in K_d does not affect the maximum enhancement in either type of titration. A change in N affects the maximum enhancement only when fluorophore is the titrant. Therefore, both cofactors must affect γ, because γ is the only parameter that affects the maximum enhancement in both types of titration.

Of course, cofactor binding could affect more than one parameter. However, in the case of TNP-ATP binding to the gastric ATPase, the percentage quench caused by either metal is approximately the same in both types of titration. Therefore, the stoichiometries estimated from the ratio of the maximum enhancements observed in titrations with fluorophore and protein are the same in the presence and absence of cofactor for both metals. Some contribution of dissociation to the observed fluorescence quenches cannot be excluded, but any change in K_d must be small. An indication of this is that the same N is estimated from $[T]_{0,1/2}$ and E_{max} values measured in the presence of cofactor.

Although the mechanisms of the cofactor-induced fluorescence quenches are the same, the protein environments induced by K^+ and Mg^{2+} are not the same. The K^+ quench is fast and is initially reversed by Mg^{2+}, which then causes a much slower quench (Figure 4). Therefore, at least three different conformational states of the enzyme are needed to explain the effects of K^+ and Mg^{2+} on the fluorescence yield of bound TNP-ATP:

$$Mg^{2+}\ (\pm K^+)\cdot E_c\cdot \text{TNP-ATP} \underset{\text{slow}}{\overset{Mg^{2+}\ (\pm K^+)}{\longleftarrow}} E_a\cdot \text{TNP-ATP} \underset{Mg^{2+},\ \text{fast}}{\overset{K^+,\ \text{fast}}{\rightleftharpoons}} K^+\cdot E_b\cdot \text{TNP-ATP}$$

Lower case letters have been used to denote these different conformers, because their relationship to E_1 and E_2 has not been established.

Conclusions about H,K-ATPase. There is extensive experimental evidence for E_1 and E_2 conformations of the Na,K-ATPase, including temporal correlation of changes in the enzyme with events in the catalytic cycle (Karlish & Yates, 1978). There is only limited and indirect evidence for conformational changes in the H,K-ATPase by comparison. The best evidence the proton transporter works the same way as the sodium transporter is that both ^{14}C exchange between ADP and ATP (Rabon et al., 1982; Helmich-de Jong et al., 1985) and ^{18}O exchange between inorganic phosphate and water (Faller & Elgavish, 1984) are catalyzed, so there must be high- and low-energy phosphoenzyme intermediates.

Only two attempts to directly observe conformational changes in the gastric enzyme have been published previously, both employing fluorescent reporter groups. In the earlier study, fluorescein irreversibly inhibited the enzyme by covalently modifying the active site (Jackson et al., 1983), so the fluorescence changes caused by cofactors may not report conformational states of the functional enzyme. In the more recent study, a conformational change was proposed to explain additional eosin binding in the presence of Mg^{2+} (Helmich-de Jong et al., 1986). TNP-ATP is the first reversible probe that has been shown to report conformational changes in the gastric enzyme directly by a change in the enhancement factor of bound fluorophore. Therefore, an important result of this study is the most direct evidence to date for cofactor-induced conformational changes in the functional H,K-ATPase.

The eosin study (Helmich-de Jong et al., 1986) illustrates the importance (and difficulty) of establishing the mechanism of a ligand-induced fluorescence change. The fluorescence enhancement caused by Mg^{2+} was explained by an increase in the number of eosin binding sites. Direct binding measurements reported in the paper seem to support this interpretation. However, when fluorescence titrations of eosin with protein in Mg^{2+} and in K^+ were compared, the maximum enhancement was approximately twice as great in Mg^{2+} [Figure 4 in Helmich-de Jong et al. (1986)]. Since all of the fluorophore is bound at the end point of a titration with protein, the observed increase in E_{max} cannot be explained by an increase in the number of sites alone (or in combination with a change in binding affinity). An increase in enhancement factor is the only possible explanation of an increase in E_{max} when protein is titrant. Therefore, the published interpretation

of the fluorescence titrations is wrong, and the inference that Mg^{2+} increases the number of eosin binding sites on the H,K-ATPase may be incorrect.

Comparison with Other E_1E_2-ATPases. The conclusion drawn from the study of TNP-ATP binding to Na,K-ATPase was that metal cofactors shift the equilibrium between the E_1 and E_2 conformers of the enzyme, which have different affinities for TNP-ATP (Moczydlowski & Fortes, 1981). This conformational shift in nucleotide affinity has been used to explain activation of the sodium pump by high concentrations of ATP without invoking a second active site (Cantley et al., 1978).

Since a different conclusion has been reached in this study of TNP-ATP binding to the H,K-ATPase, it is important to emphasize that fundamentally different experimental results were obtained with the two enzymes. In contrast to the titrations of H,K-ATPase with TNP-ATP pictured in Figure 2, the same maximum enhancement was observed when Na,K-ATPase was titrated with TNP-ATP in the presence of K^+, but more TNP-ATP was required to reach saturation than in the absence of the monovalent cation (Moczydlowski & Fortes, 1981). Therefore, in the case of the Na,K-ATPase the underlying mechanism of the cofactor-induced fluorescence quench is reduced affinity for TNP-ATP, while in the case of the H,K-ATPase it is a change in the enhancement factor. A shift in nucleotide affinity is not needed to explain the changes in TNP-ATP fluorescence caused by K^+ or Mg^{2+} binding to the H,K-ATPase.

The stoichiometry of TNP-ATP binding to the Na,K-ATPase equaled the stoichiometry of ouabain binding (Moczydlowski & Fortes, 1981), and the latter equals the stoichiometry of phosphoenzyme formation (Peters et al., 1981). In sharp contrast, the stoichiometry of TNP-ATP binding to the H,K-ATPase is twice the phosphorylation stoichiometry. I have discussed this result along with other evidence for two sites, instead of two states of a single nucleotide site, in a recent paper describing competitive binding of TNP-ATP and ATP to the H,K-ATPase (Faller, 1989a).

The stoichiometry of TNP-nucleotide binding to SR Ca-ATPase is approximately twice the phosphorylation capacity of the enzyme in all but one account (Dupont et al., 1982, 1985; Wanatabe & Inesi, 1982; Nakamoto & Inesi, 1984; Bishop et al., 1984, 1987). Phoshorylation of the Ca-ATPase causes a large, additional enhancement of bound TNP-nucleotide fluorescence that has been explained by a different conformation of the phosphoenzyme (Dupont & Pougeois, 1983; Nakamoto & Inesi, 1984; Bishop et al., 1984; Berman, 1986). Enhanced TNP-nucleotide fluorescence under phosphorylating conditions was not reported for the Na,K-ATPase (Moczydlowski & Fortes, 1981), nor is it observed with the H,K-ATPase (Faller, 1989a).

In a general way studies with the fluorescent substrate analogue TNP-ATP support the E_1E_2 model of active transport. There is unequivocal evidence for protein conformational changes that are affected by the transported ions. At the same time it is important to keep in mind that fundamentally different results have been obtained by using the same probe to report conformational changes in three members of the E_1E_2 class. The mechanism of cofactor-induced changes in the Na,K-ATPase and H,K-ATPase is different; TNP-ATP reports a conformational change caused by phosphorylation in only one of the enzymes (Ca-ATPase). The convention of designating conformations of all three enzymes in the same way obscures the possibility that TNP-ATP may report different reactions in the three enzymes and that the conformational changes being studied may not all be related to the E_1–E_2 transition in the model which explains energy coupling and ion transport.

Acknowledgments

I am indebted to Terry J. Reedy for help with the statistical analysis, to Giorgio Sartor, Gaetano Saccomani, and George Sachs for access to their unpublished work, and to Dr. Sachs for organizing the program project that provided partial support for the initial phase of this investigation.

Appendix

The observed fluorescence (F_{obs}) is the sum of the contributions of free and bound fluorophore and an apparent fluorescence that is really scattered light:

$$F_{obs} = F_{free} + F_{bound} + F_{scatter} \quad (4)$$

To a first approximation the contributions of free fluorophore and of light scattering to the signal are proportional to their concentrations:

$$F_{free} = Q[L] \quad (5)$$

$$F_{scatter} = RP_0 \quad (6)$$

Q and R are constants of proportionality. The fluorescence of bound fluorophore can be expressed as

$$F_{bound} = \gamma Q[SL] \quad (7)$$

where [SL] is the concentration of filled sites. The enhancement factor (γ) is the ratio of fluorescence intensities when the same amount of fluorophore is bound and free. Combining eqs 5–7 with eq 4 and rearranging gives

$$F_{obs} = (Q[L]_0 + RP_0) + (\gamma - 1)Q[SL] \quad (8)$$

since

$$[L]_0 = [L] + [SL] \quad (9)$$

In the special case of ligand binding to a single class of N identical and independent protein sites ($[S]_0 = NP_0$) with dissociation constant K_d, substituting the conservation of mass equations into the expression for K_d and rearranging result in a quadratic equation:

$$[SL]^2 - ([L]_0 + NP_0 + K_d)[SL] + NP_0[L]_0 = 0 \quad (10)$$

Only one solution of eq 10 is physically possible. Introduction of the "minus discriminant" solution into eq 8 gives eq 1.

References

Berman, M. C. (1986) *J. Biol. Chem. 261*, 16494–16501.
Bishop, J. E., Johnson, J. D., & Berman, M. C. (1984) *J. Biol. Chem. 259*, 15163–15171.
Bishop, J. E., Al-Shawi, M. K., & Inesi, G. (1987) *J. Biol. Chem. 262*, 4658–4663.
Cantley, L. C., Jr., Cantley, L. G., & Josephson, L. (1978) *J. Biol. Chem. 253*, 7361–7368.
Chang, H., Saccomani, G., Rabon, E., Schackmann, R., & Sachs, G. (1979) *Biochim. Biophys. Acta 464*, 313–327.
Dupont, Y., & Pougeois, R. (1983) *FEBS Lett. 156*, 93–98.
Dupont, Y., Chapron, Y., & Pougeois, R. (1982) *Biochem. Biophys. Res. Commun. 106*, 1272–1279.
Dupont, Y., Pougeois, R., Ronjat, M., & Verjovsky-Almeida, S. (1985) *J. Biol. Chem. 269*, 7241–7249.
Faller, L. D. (1986) *Biophys. J. 49*, 38a.
Faller, L. D. (1989a) *Biochemistry 28*, 6771–6778.
Faller, L. D. (1989b) *Biochemistry 28*, 6908–6914.
Faller, L. D., & Elgavish, G. A. (1984) *Biochemistry 23*, 6584–6590.

Faller, L. D., Rabon, E., & Sachs, G. (1983) *Biochemistry 22*, 4676-4685.
Farley, R. A., & Faller, L. D. (1985) *J. Biol. Chem. 260*, 3899-3901.
Ganser, A. L., & Forte, J. G. (1973) *Biochim. Biophys. Acta 307*, 169-180.
Helmich-de Jong, M. L., van Emst-de Vries, S. E., De Pont, J. J. H. H. M., Schuurmans Stekhoven, F. M. A. H., & Bonting, S. L. (1985) *Biochim. Biophys. Acta 821*, 377-383.
Helmich-de Jong, M. L., van Duynhoven, J. P. M., Schuurmans Stekhoven, F. M. A. H., & De Pont, J. J. H. H. M. (1986) *Biochim. Biophys. Acta 858*, 254-262.
Hiratsuka, T. (1982) *Bichim. Biophys. Acta 719*, 509-517.
Hiratsuka, T., & Uchida, K. (1973) *Biochim. Biophys. Acta 320*, 635-647.
Jackson, R. J., Mendlein, J., & Sachs, G. (1983) *Biochim. Biophys. Acta 731*, 9-15.
Jencks, W. P. (1980) *Adv. Enzymol. 51*, 75-106.
Karlish, S. J. D., & Yates, D. W. (1978) *Biochim. Biophys. Acta 527*, 115-130.
Lowry, O. H., Rosenbrough, N. J., Farr, A. L., & Randall, R. J. (1951) *J. Biol. Chem. 193*, 265-275.
MacLennan, D. H., Brandl, C. J., Korczak, B., & Green, N. M. (1985) *Nature 316*, 696-700.
Moczydlowski, E. G. & Fortes, P. A. G. (1981) *J. Biol. Chem. 256*, 2346-2356.
Nakamoto, R. K., & Inesi, G. (1984) *J. Biol. Chem. 259*, 2961-2970.
Peters, W. H. M., Swarts, H. G. P., de Pont, J. J. H. H. M., Schuurmans Stekhoven, F. M. A. H., & Bonting, S. L. (1981) *Nature 290*, 338-339.
Rabon, E. C., Sachs, G., Mardh, S., & Wallmark, B. (1982) *Biochim. Biophys. Acta 688*, 515-524.
Rabon, E., Gunther, R. D., Soumaron, A., Bassilian, S., Lewin, M., & Sachs, G. (1985) *J. Biol. Chem. 260*, 10200-10207.
Sartor, G., Mukidjam, E., Faller, L., Saccomani, G., & Sachs, G. (1982) *Biophys. J. 37*, 375a.
Shull, G. E., & Lingrel, J. B. (1986) *J. Biol. Chem. 261*, 16788-16791.
Shull, G. E., Schwartz, A., & Lingrel, J. B. (1985) *Nature 316*, 691-695.
Tanford, C. (1983) *Annu. Rev. Biochem. 52*, 379-409.
Walderhaug, M. O., Post, R. L., Saccomani, G., Leonard, R. T., & Briskin, D. P. (1985) *J. Biol. Chem. 260*, 3852-3859.
Wallmark, B., & Mardh, S. (1979) *J. Biol. Chem. 257*, 11899-11902.
Wanatabe, T., & Inesi, G. (1982) *J. Biol. Chem. 257*, 11510-11516.

Stabilization of a Reaction Intermediate as a Catalytic Device: Definition of the Functional Role of the Flexible Loop in Triosephosphate Isomerase†

David L. Pompliano,‡ Anusch Peyman,§ and Jeremy R. Knowles*
Department of Chemistry, Harvard University, Cambridge, Massachusetts 02138
Received September 15, 1989; Revised Manuscript Received December 11, 1989

ABSTRACT: The function of the mobile loop of triosephosphate isomerase has been investigated by deleting four contiguous residues from the part of this loop that interacts directly with the bound substrate. From the crystal structure of the wild-type enzyme, it appears that this excision will not significantly alter the conformation of the rest of the main chain of the protein. The specific catalytic activity of the purified mutant enzyme is nearly 10^5-fold lower than that of the wild type. Kinetic measurements and isotopic partitioning studies show that the decrease in activity is due to much higher activation barriers for the enolization of enzyme-bound substrate. Although the substrates bind somewhat more weakly to the mutant enzyme than to the wild type, the intermediate analogue phosphoglycolohydroxamate binds much less well (by 200-fold) to the mutant. It seems that the deleted residues of the loop contribute critically to the stabilization of the enediol phosphate intermediate. Consistent with this view, the mutant enzyme can no longer prevent the loss of the enediol phosphate from the active site and its rapid decomposition to methylglyoxal and inorganic phosphate. Indeed, when glyceraldehyde 3-phosphate is the substrate, the enediol phosphate intermediate is lost (and decomposes) 5.5 times faster than it reprotonates to form the product dihydroxyacetone phosphate. Triosephosphate isomerase has evidently evolved its mobile loop to bind tightly the highly reactive intermediate enediol phosphate, in a conformation that disfavors the wasteful elimination process. These studies support the increasing recognition of the essential function (as distinct from the mere existence) of mobile loops near the active sites of enzymes.

Loops pervade the proteins of known structure (Leszcynski & Rose, 1986; Richardson, 1981). Considered to be nonregular elements of protein secondary structure, loops are contiguous segments of polypeptide, variable in size and sequence, that trace a curved path through space. Loops may exist in a range of conformations and have a relatively small end-to-end distance separating the segment termini. The side chains of loop residues are usually hydrophilic and are almost always situated on the protein surface where they are well placed to interact with ligands such as substrates, hormones, and effectors.

The question of whether loops have a functional role in ligand recognition or in enzyme catalysis is not one that has often received direct experimental support, despite the existence

† This work was supported by the National Institutes of Health and Merck Sharp & Dohme.
‡ National Institutes of Health Postdoctoral Fellow.
§ Present address: Hoechst AG, Pharma Synthese G838, Postfach 800320, 6230 Frankfurt 80, West Germany.

0006-2960/90/0429-3186$02.50/0